Proceedings of ASME Turbo Expo 2011
GT2011
June 6-10, 2011, Vancouver, British Columbia, Canada

GT2011-46710

Characterization of Pre- and Post-Service Grain Boundary Phases in a Cast Austenitic Steel

Raymond R. Unocic,[1] Kinga A. Unocic,[1] Bruce A. Pint,[1] and Mark D. Lipschutz[2]

[1]Materials Science and Technology Division
Oak Ridge National Laboratory
Oak Ridge, TN 37831

[2] Solar Turbines Incorporated
San Diego, CA 92186

ABSTRACT

Austenitic steel castings are currently being used in components for industrial gas turbine engines. Service experience has indicated a degradation of mechanical properties with extended exposures at elevated temperature. The purpose of this study was to characterize the grain boundary phases that develop during the casting processes as a likely explanation for the observed performance. In order to isolate these precipitates, a variety of electron microscopy characterization techniques were used to characterize their composition after various heat treatments and service exposure. In the baseline, as-cast and annealed condition, a discontinuous network of grain boundary metal carbides was observed. These precipitates coarsened during short-term annealing at 649°C and a denuded zone formed in the adjacent matrix. When the 38,600 h service-exposed material was analyzed, the grain boundaries were highly decorated with a more continuous film of grain boundary carbides as well as voids attributed to creep cavitation. In addition to carbides, acicular AlN precipitates were identified on the grain boundaries of the casting examined after service exposure.

INTRODUCTION

Ductile cast austenitic steels are currently being used in industrial gas turbine engine applications in components such as housings, stators, compressors and exhaust diffusers where elevated temperature strength, ductility, wear and corrosion resistance are the main material property requirements. This class of alloys is typically known as Ni-Resist alloys, where a relatively high amount of Ni is added in order to stabilize the austenite structure so the materials can be utilized in higher temperature applications as compared to their ferritic grade ductile steel counterparts. For specific applications where a combination of low thermal expansion, dimensional stability, and structural integrity is needed during service at elevated temperature, the ASTM 439 Type D5 alloy is generally used [1]. In order to improve upon the corrosion resistance and mechanical properties (e.g., creep rupture life) of the baseline D5 alloy, elements such as chromium and molybdenum are intentional added which has formed the basis of the D5B+Mo (containing 1% Mo) alloy. Depending upon the carbon content, the microstructure can contain graphite particles with nodule or flake-like morphology, which are dispersed in the austenitic iron matrix. Recently, there has been the desire to modify the baseline D5B+Mo alloy composition to eliminate the formation of the graphite nodules, and to further refine the mechanical properties [2]. An alloy development program by Solar Turbines Incorporated and Wollaston alloys modified the baseline D5B+Mo alloy by decreasing the carbon content. A comparison of the chemical compositions between the modified DX35BM and the baseline D5B+Mo alloys is shown in Table I. The chemical composition ranges of the primary alloying elements such as nickel, chromium, molybdenum and silicon have not been altered while the carbon content has been decreased significantly. The dramatic reduction in carbon content inhibited the formation of nodular graphite [2].

Table I. Chemical composition specification for cast austenitic steel alloy DX35BM and D5B+Mo [2].

Element	DX35BM (wt.%)	D5B + Mo (wt.%)
Carbon	0.22-0.30	2.40 (max)
Silicon	1.54-1.90	1.00-2.80
Manganese	0.55-0.69	0.40-1.00
Phosphorus	0.006-0.019	0.08 (max)
Nickel	34.10-36.00	34.00-36.00
Chromium	2.10-3.00	2.00-3.00
Molybdenum	0.76-1.00	0.70-1.00
Sulfur	0.001-0.010	N/A
Iron	Bal.	Bal.

Solar Turbines Incorporated has been using DX35BM in industrial gas turbine engine applications. The purpose of this study was to develop a better understanding of the alloy microstructural evolution during long-term elevated temperature service. The microstructures of pre- and post-service conditions were characterized, with an emphasis on phase transformations, especially at grain boundaries, that may be responsible for the observed degradation in mechanical properties [3].

EXPERIMENTAL PROCEDURE

The austenitic steel DX35BM alloy used in this study was cast by Wollaston alloys and was characterized in the pre-service, as-cast condition and in the post-service condition. Table II shows the material conditions that were characterized. Specimens for materials characterization were extracted from the castings and metallographically prepared using standard procedures.

Table II. Experimental test conditions for cast austenitic DX35BM alloy used in this study.

Specimen ID	Condition
DX35BM-I	As Cast, Annealed (1675°F/1 h)
DX35BM-III	As Cast + Anneal + Furnace Exposed (1200°F/500 h)
DX35BM-IV	Service Exposed (1200°F/38,600 h)

A combination of light optical microscopy (LOM), scanning electron microscopy (SEM), and transmission electron microscopy (TEM) was used for microstructural characterization. For LOM, specimens were etched with a 2% nital solution to reveal the microstructure, while specimens for SEM and microprobe analysis were studied in the as-polished condition. A Hitachi model S3400 SEM equipped with an EDAX energy dispersive spectrometer (EDX) system was used to characterize the grain boundary phases. Specimens for TEM characterization were prepared using a Hitachi model NB5000 focused ion beam (FIB) instrument. TEM and EDX analysis was performed on a Phillips model CM200 equipped with a Schottky field emission gun (FEG) operating at 200 kV.

RESULTS and DISCUSSION

As-cast/Annealed Microstructure

The microstructure of the DX35BM steel castings in the as-cast/annealed condition is shown in Figure 1. Following casting, the material was subjected to an annealing heat treatment at 913°C (1675°F) for 1 h, which transformed the solidification substructure and resulted in the formation of equiaxed grains. The higher magnification image in Figure 1b revealed that the grain boundaries are highly decorated with a discontinuous network of grain boundary precipitates. A fine dispersion of precipitates was observed within the austenite matrix with two distinct morphologies: globular and acicular. The density of these precipitates varied by location within the casting but precipitates were observed along all of the grain boundaries.

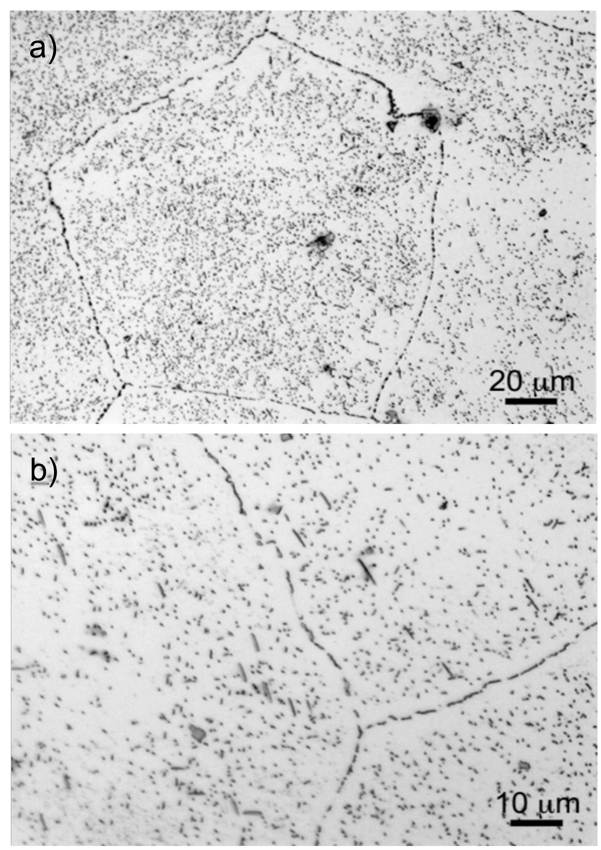

Figure 1. Light optical micrographs of the DX35BM alloy in the as cast/annealed condition showing a) equiaxed austenite grains with a fine dispersion of matrix precipitates and b) grain boundaries enriched in a discontinuous network of precipitates.

Since intergranular cracking was reported [3], an emphasis was placed on characterizing the structure and chemistry of the grain boundary precipitate phases. A representative SEM image from a grain boundary triple point is shown in Figure 2 along with a point EDX spectrum of the precipitate marked in Figure 2a. Due to the electron beam size relative to the precipitates, there is a significant contribution of x-rays that are generated from the matrix phase; however, EDX elemental mapping (Figure 3) of this area qualitatively shows that the grain boundary precipitates are enriched in chromium, molybdenum, manganese, and carbon, which suggests that there are several forms of metal carbides [4]. Based on these results, Cr rich $M_{23}C_6$ carbides and Mo rich Mo_2C carbides are present. Higher resolution characterization was necessary to quantitatively characterize the precipitate composition.

Thin TEM foils prepared by FIB along a grain boundary provided a more in depth analysis of the grain boundary precipitates phases. A representative HAADF STEM image of a typical grain boundary is shown in Figure 4.

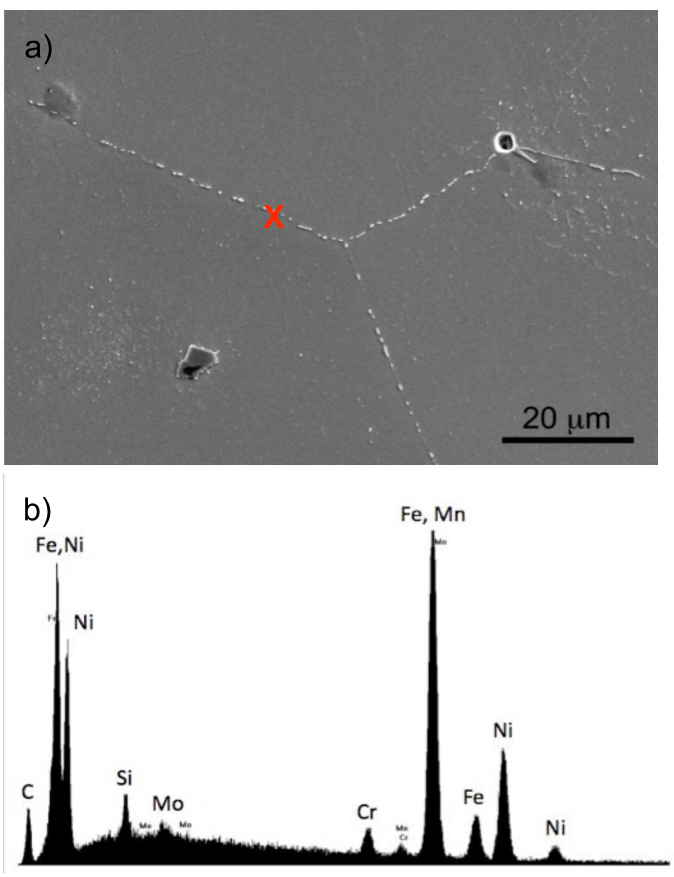

Figure 2. a) Representative SEM micrograph of DX35BM in the as cast plus annealed condition revealing a discontinuous network of grain boundary phases and b) corresponding point EDX spectrum from location X.

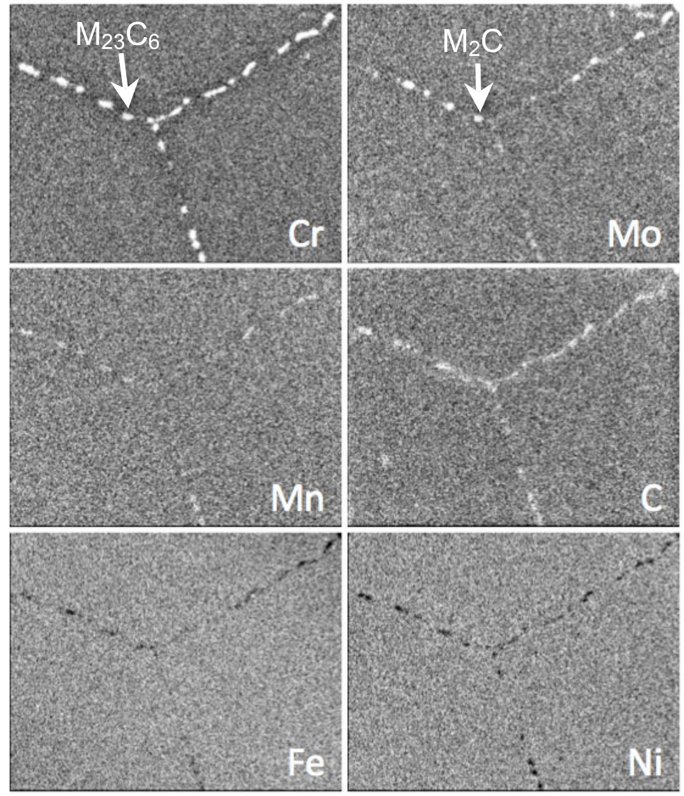

Figure 3. Qualitative EDX elemental maps from the grain boundary triple point of DX35BM (Figure 2) showing the discontinuous network of grain boundary precipitates which are enriched in Cr, Mo, Mn and C.

Through a combination of point EDX, EDX line profiles, and selected area electron diffraction (SAED), distinct phases were indentified: metal carbides and manganese sulfides. The EDX line profiles across two precipitates are shown in Figure 4b-c. Enrichment of Cr and C in line scan 1 (Fig. 4b) gives clear indication that this is a $M_{23}C_6$ type chromium carbide. The inset selected area diffraction pattern acquired along the [111] zone axis of another embedded carbide provides further confirmation of the $M_{23}C_6$ type structure of the carbides. In addition to the metal carbides, there are also MnS inclusions that are present, which can clearly be seen in line scan 2 (Fig. 4c).

Lab Exposed Microstructure

To better understand how the microstructure evolved during exposure, the as cast/annealed specimens were heat treated at 649°C (1200°F) for 500 h in a laboratory furnace. The typical microstructure following this exposure is shown in Figure 5. It is evident that the discontinuous grain boundary phase present after casting and annealing has become more continuous and a matrix precipitate denuded zone has appeared along the boundaries.

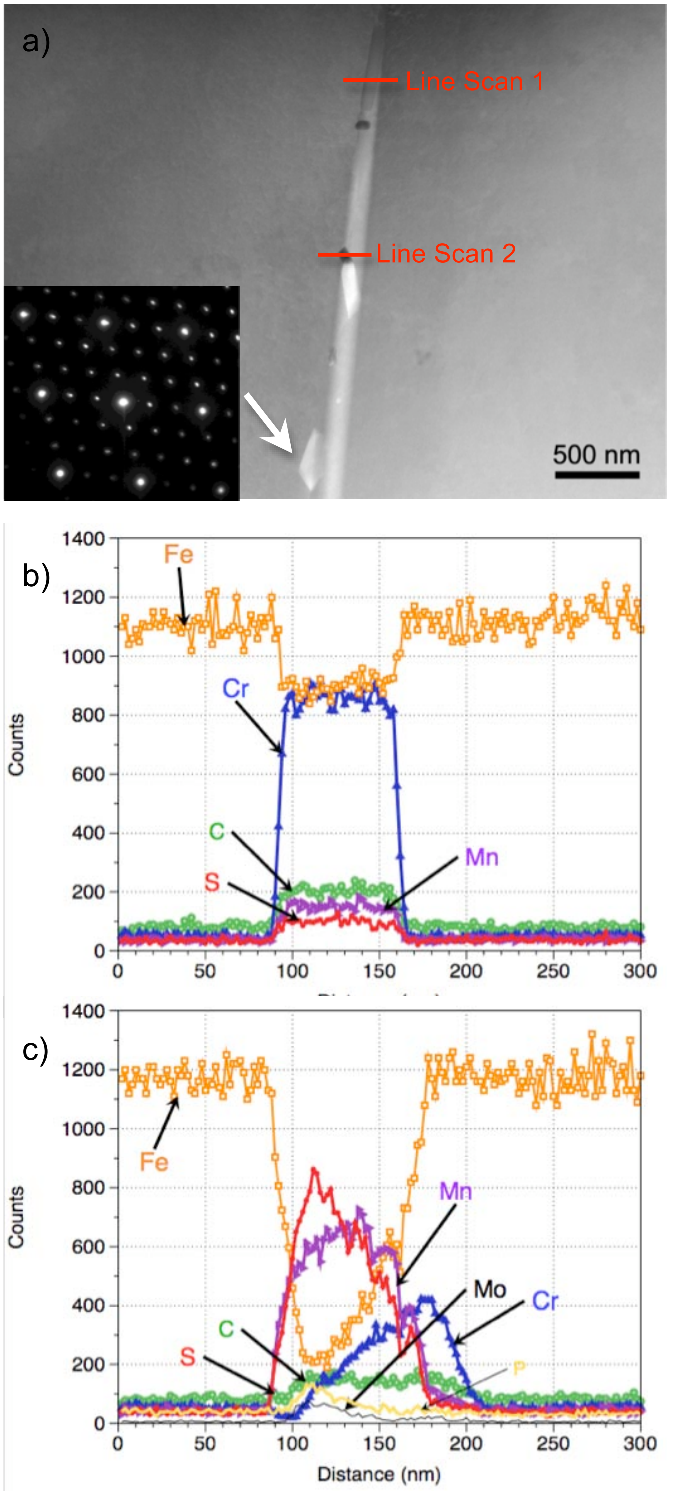

Figure 4. a) HAADF STEM image of a FIB prepared cross section from a typical grain boundary, b) EDX line scan 1 and c) EDX line scan 2. (Inset SAED pattern of a $M_{23}C_6$ type carbide)

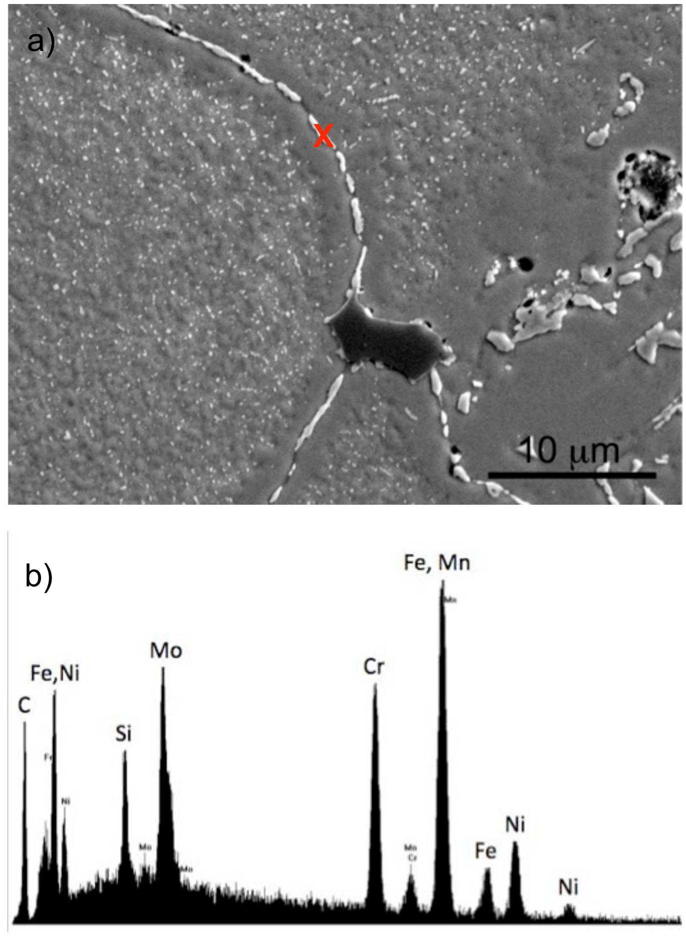

Figure 5. a) Representative SEM micrograph of DX35BM following thermal exposure at 1200F for 500hrs and b) point EDX spectrum from the grain boundary marked X.

The EDX spectrum from these grain boundary preciptiates in Figure 5b is similar to that shown in Figure 2b, however, the peaks corresponding to Cr, Mo, and C are more intense. In general, this can be attributed to more x-rays originating from these larger precipitates suggesting a similar precipitate composition as after casting and annealing. As these results suggested that the 649°C anneal mainly resulted in grain boundary particle coarsening, no additional TEM was performed on this specimen.

Service Exposed Microstructure

Following exposure under service conditions at 38,600 hrs, LOM and SEM characterization revealed voids at a majority of the grain boundaries. Figure 6 is a typical example. The appearance of the voids does not suggest casting porosity or precipitate pull out during metallographic polishing. It was concluded that these voids formed in service and are likely creep cavitation voids.

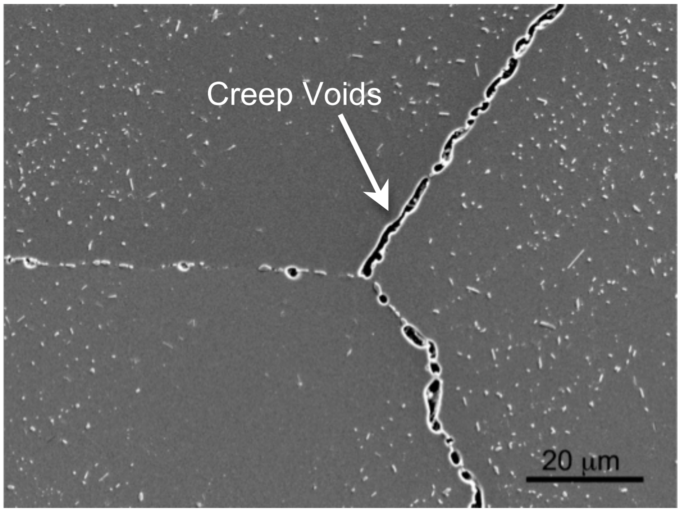

Figure 6. Representative SEM micrograph showing grain boundary creep void formation after 38,600 h service.

More detailed TEM characterization was performed to further study the precipitates after service exposure. A FIB prepared TEM foil was extracted across a grain boundary in a region that did not have a high density of grain boundary voids and a somewhat discontinuous network of grain boundary phases. A HAADF STEM image of the grain boundary is shown in Figure 7a. TEM EDX spot analysis was used to confirm the presence of grain boundary $M_{23}C_6$ type chromium carbides. In addition to the main carbides that were present, rod shaped grain boundary precipitates also were observed. EDX line scans (Figure 7b) showed these to be aluminum nitride (AlN). Further work is needed to confirm this observation in other service-exposed castings and determine the Al and N contents of the alloy leading to their formation.

The presence of nitrides as well as carbides in the service-exposed material increases the number of possible explanations for the observed degradation in mechanical properties in long-term service [4]. Lillo et al. [5] has reported that $M_{23}C_6$ carbides alone can affect the creep resistance of Ni-base alloy 617 and that creep void formation is often associated with grain boundary character and carbides. Furthermore, if these precipitates can explain the observations, mitigation strategies can be investigated. Recently, Zangeneh has shown that it may be possible to recover some ductility with a rejuvenation heat treatment that alters the carbide morphology [6].

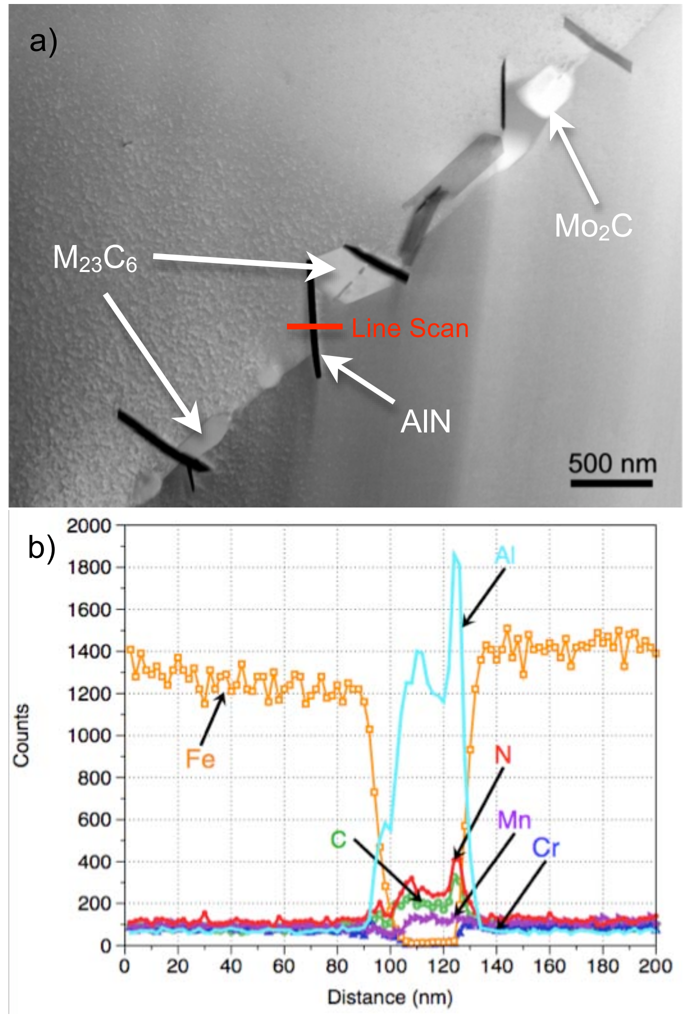

Figure 7. a) HAADF STEM image from the a FIB prepared cross section showing the grain boundary precipitates in the service exposed material and b) corresponding EDX line scan which was identified to be AlN.

CONCLUSIONS

This study has shown that after casting and annealing, the grain boundaries of alloy DX35BM are enriched in a discontinuous network of carbides. Through detailed characterization of these phases, it was determined that $M_{23}C_6$ type metal carbides were the dominant phase. Following annealing at 649°C for 500h, these carbides coarsened forming a more continuous grain boundary film. Also, a precipitate-denuded zone formed in the adjacent matrix. After service at a similar temperature for 38,600 h, grain boundary voids were observed that were attributed to cavitation due the service stress. The grain boundaries contained both $M_{23}C_6$ type metal carbides and acicular AlN precipitates after service. Further work is needed to confirm these observations and understand the effect of these grain boundary phases on the long-term properties of this alloy.

ACKNOWLEDGEMENTS

The authors would like to acknowledge the technical assistance of Tracie Brummett, Dorothy Coffey, Hu Longmire, Larry Walker, and Kathy Powers at Oak Ridge National Laboratory. Research sponsored by the U.S. Department of Energy, Assistant Secretary for Energy Efficiency and Renewable Energy, Industrial Technologies Program (Combined Heat and Power).

REFERENCES

1. Davis J.R., Cast Irons, ASM Specialty Handbook, 1996, pg 54.
2. Neyhouse, J.R., Aurrecoechea, J.M., Montague J.P., "Cast Iron-Nickel Alloy for Industrial Gas Turbine Engine Applications," ASME Paper #GT2005-68837, presented at the International Gas Turbine & Aeroengine Congress & Exhibition, Reno-Tahoe, NV, June 6-9 (2005).
3. Internal Report, 2010, Solar Turbines Inc., San Diego, CA.
4. Kaneko, K., Matsumura, S., Sadakata, A., Fujita, K., Moon, W.J., Ozaki, S., Nishimura, N., Tomokiyo, Y., "Characterization of carbides at different boundaries of 9Cr-steel," Materials Science and Engineering A, 374 (2004) 82-89.
5. Lillo, T., Cole, J., Frary, M. Schlegel, S., Influence of Grain Boundary Character on Creep Void Formation in Alloy 617," Metallurgical and Materials Transactions A, 40 (2009) 2803-2811.
6. Zangeneh, S., Farhangi, H., Lashgari, H.R., "Rejuvenation of degraded first stage gas turbine nozzle by heat treatment," Journal of Alloys and Compounds, 497 (2010) 360-368.